Research Article | Vol. 29, No. 24 / 22 Nov 2021 / Optics Express 40323
Optics EXPRESS

SWCNT-SA mode-locked Tm,Ho:LCLNGG laser

Zhongben Pan,[1,2,3] Li Wang,[1,*] Ji Eun Bae,[4] Fabian Rotermund,[4] Yicheng Wang,[5] Yongguang Zhao,[6] Pavel Loiko,[7] Xavier Mateos,[8] Uwe Griebner,[1] Valentin Petrov,[1] and Weidong Chen[1,2]

[1]*Max Born Institute for Nonlinear Optics and Short Pulse Spectroscopy, Max-Born-Str. 2a, 12489 Berlin, Germany*
[2]*Fujian Institute of Research on the Structure of Matter, Chinese Academy of Sciences, 350002 Fuzhou, China*
[3]*Institute of Chemical Materials, China Academy of Engineering Physics, 621900 Mianyang, China*
[4]*Department of Physics, Korea Advanced Institute of Science and Technology (KAIST), 34141 Daejeon, Republic of Korea*
[5]*Photonics and Ultrafast Laser Science, Ruhr Universität Bochum, Universitätsstraße 150, 44801 Bochum, Germany*
[6]*Jiangsu Key Laboratory of Advanced Laser Materials and Devices, Jiangsu Normal University, 221116 Xuzhou, China*
[7]*Centre de Recherche sur les Ions, les Matériaux et la Photonique (CIMAP), UMR 6252 CEA-CNRS-ENSICAEN, Université de Caen, 6 Boulevard Maréchal Juin, 14050 Caen Cedex 4, France*
[8]*Universitat Rovira i Virgili, Física i Cristal·lografia de Materials i Nanomaterials (FiCMA-FiCNA)-Marcel·lí Domingo 1, 43007, Tarragona, Spain*
[*]*Li.Wang@mbi-berlin.de*

Abstract: Sub-100 fs pulse generation from a passively mode-locked Tm,Ho-codoped cubic multicomponent disordered garnet laser at ~2 μm is demonstrated. A single-walled carbon nanotube saturable absorber is implemented to initiate and stabilize the soliton mode-locking. The Tm,Ho:LCLNGG (lanthanum calcium lithium niobium gallium garnet) laser generated pulses as short as 63 fs at a central wavelength of 2072.7 nm with an average output power of 63 mW at a pulse repetition rate of ~102.5 MHz. Higher average output power of 121 mW was obtained at the expense of longer pulse duration (96 fs) at 2067.6 nm using higher output coupling. To the best of our knowledge, this is the first report on mode-locked operation of the Tm,Ho:LCLNGG crystal.

1. Introduction

Mode-locked solid-state lasers emitting sub-100-fs pulses in the 2-μm spectral range featuring relatively high average output powers (above 100 mW) at high repetition rates (about 100 MHz) and Fourier-transform limited pulses with sideband-free spectra are very suitable for applications as frequency combs in high resolution molecular spectroscopy [1] as well as for seeding/pumping of parametric nonlinear frequency down-conversion [2] and ultrafast (chirped-pulse) regenerative laser amplifiers [3]. Typically, solid-state laser emission at ~2 μm is achieved using thulium (Tm^{3+}) or holmium (Ho^{3+}) ions. Recently, significant efforts were applied towards exploring and developing novel laser materials featuring broad and smooth spectral gain profiles naturally extending beyond 2 μm which is desirable to avoid the detrimental water vapor absorption/dispersion in the atmosphere.

Typically, Tm lasers tend to operate slightly below 2 μm (on the $^3F_4 \rightarrow {}^3H_6$ electronic transition), which requires a special spectrally selective element to red-shift the oscillation wavelength above 2 μm for generating femtosecond pulses from mode-locked (ML) lasers [4]. Obviously, such a spectrally selective element will limit the achievable emission bandwidth

#445584 https://doi.org/10.1364/OE.445584
Journal © 2021 Received 22 Oct 2021; revised 3 Nov 2021; accepted 4 Nov 2021; published 17 Nov 2021

Optics EXPRESS

and, thus, the minimum pulse duration. In order to overcome this limitation, few crystalline matrices have been identified, either featuring strong crystal fields for the Tm^{3+} ions causing to a large total Stark splitting of the ground-state ($^3H_6$) or structural/compositional disorder leading to significant inhomogeneous spectral broadening resulting in extremely broad and flat gain profiles extending up to 2.1 μm. Large crystal field splitting combined with disorder is characteristic of some families of isotropic materials, such as the cubic multicomponent garnets (e.g. $Ca_3Nb_{1.5}Ga_{3.5}O_{12}$-type) [5,6], and the mixed cubic rare-earth sesquioxides A_2O_3 (where A is a combination of Sc, Y and Lu) [7–10].

Alternatively, by doping with Ho^{3+} instead of Tm^{3+} ions, one can ensure laser oscillation wavelengths above 2 μm on the $^5I_7 \rightarrow {}^5I_8$ transition independent of the host material, together with higher gain cross-sections in this spectral range. However, Ho^{3+}-doped crystalline laser gain media exhibit narrower and structured gain profiles which limits the achievable spectral bandwidth in femtosecond ML lasers. With respect to direct diode pumping, AlGaAs-based laser diodes emitting near 0.8 μm for Tm-doped materials are well developed and widely commercially available whereas the required InP-based laser diodes with emission around 1.9 μm for Ho pumping have not yet reached a mature level. Besides, high-brightness tunable continuous-wave (CW) pump sources for Ho lasers are still not well developed. Tm^{3+}, Ho^{3+}-codoped gain media provide a certain trade-off in terms of spectroscopic properties given the advantages and limitations of the two dopants. In a codoped material, the composite gain profile depends on the individual emission and reabsorption cross-sections and the corresponding inversion rates. Consequently, Tm,Ho-codoped laser materials are expected to support extremely broad spectra (i.e., corresponding to few optical-cycle pulses). Inhomogeneous spectral broadening in disordered host materials can be exploited also in the case of codoping. The first sub-100 fs pulse generation using a codoped material was reported in 2018. A Tm,Ho-codoped disordered tetragonal $CaYAlO_4$ crystal was employed as a gain medium and 87-fs pulses at ~2043 nm with an average output power of 27 mW were generated using a GaSb-based SEmiconductor Saturable Absorber Mirror (SESAM) [11]. Even shorter pulse duration of 52 fs was achieved from a SESAM ML isostructural Tm,Ho:$CaGdAlO_4$ laser with an average output power of 376 mW at 2015 nm [12]. Finally, pulses as short as 46 fs were emitted from a SESAM ML Tm,Ho:$Ca(Gd,Lu)AlO_4$ laser at 2033 nm with an average output power of 121 mW, combining structural and compositional disorder [13].

The cubic multicomponent garnets have already been employed as disordered host crystals for generation of ultrashort pulses from ML lasers based on Nd^{3+}, Yb^{3+} and Tm^{3+} [14–16]. Among them, the above-mentioned calcium niobium gallium garnets (abbreviated CNGG) attract significant attention because they exhibit a considerable inhomogeneous spectral line broadening for the rare-earth (RE^{3+}) dopant ions due to the local structural disorder originating from the random distribution of Nb^{5+} and Ga^{3+} cations over two non-equivalent lattice sites. The actual composition of CNGG-type crystals deviates from the stoichiometry and monovalent cations such as Na^+ or Li^+ are added (the host crystals are then abbreviated as CNNGG and CLNGG, respectively) to minimize vacancies on the structure and/or to increase the segregation coefficient of the active ion [17]. Codoping with Tm^{3+} and Ho^{3+} ions of such crystals for obtaining broadband emission properties has been described in [18]. The first sub-100 fs Tm,Ho:CNGG laser, ML by a single-walled carbon nanotube saturable absorber (SWCNT-SA), was demonstrated also in 2018. It generated 76 fs pulses at 2081 nm with an average output power of 67 mW [19]. A shorter pulse duration of 67 fs at 2083 nm was obtained from a Tm,Ho:CLNGG laser ML by the same SA [20].

A novel Tm^{3+},Ho^{3+}-codoped CNGG-type disordered cubic multicomponent crystal containing La^{3+} and Li^+ ions both serving for local charge compensation (abbreviated: Tm,Ho:LCLNGG) was recently grown at the Institute of Chemical Materials, China Academy of Engineering

Optics EXPRESS

Physics. In this work, we explore its ultrashort pulse generation potential in the sub-100 fs time domain.

2. Crystal characterization

Lanthanum calcium lithium niobium gallium garnet codoped with Tm^{3+} and Ho^{3+} ions was grown by the Czochralski (Cz) method in argon atmosphere using an iridium crucible; the seed was oriented along the [111] axis. The starting reagents [$CaCO_3$ (purity: 4N), Nb_2O_5 (4N), Ga_2O_3 (5N) and RE_2O_3 (RE = Tm, Ho, La, 5N)] were taken according to the formula $(Tm_3Ga_5O_{12})_{0.03}(Ho_3Ga_5O_{12})_{0.005}(Ca_{2.4}La_{0.6}Li_{1.22}Nb_{1.82}Ga_{2.36}O_{12})_{0.965}$. The La^{3+} and Li^+ cations were introduced for local charge compensation in heterovalent doping (as the trivalent RE^{3+} ions are expected to replace divalent Ca^{2+} host-forming cations), improvement of the material crystallinity and elimination of unwanted cationic vacancies causing color center formation. The as-grown crystal of high optical quality was yellow colored. To improve its transparency, it was annealed in air. The annealed crystal had a very weak residual yellowish coloration.

The actual concentrations of RE^{3+} ions in the crystal were determined by the inductively coupled plasma mass spectrometry (ICP – MS) method to be 2.02 at.% Tm^{3+}, 0.36 at.% Ho^{3+} and 9.87 at.% La^{3+} (all defined with respect to Ca^{2+}). The ion densities of laser-active dopants in the crystal were $N_{Tm} = 2.47 \times 10^{20}$ at/cm^3 and $N_{Ho} = 0.438 \times 10^{20}$ at/cm^3.

The crystal structure was determined by X-ray diffraction. Tm,Ho:LCLNGG belongs to the cubic class (sp. gr. $Ia\bar{3}d - O_h^{10}$, $a = 12.5292(8)$ Å, $V = 1966.88$ Å^3, Z = 8). The general chemical formula of multicomponent garnets reads $A[B]_2(C)_3O_{12}$, where A, [B] and (C) designate dodecahedral (Wyckoff symbol: 24*c*), octahedral (16*a*), and tetrahedral (24*d*) sites whose coordination numbers with oxygen, C.N. are VIII, VI and IV, respectively. The $Ca^{2+}|RE^{3+}$ cations occupy the A sites, the Nb^{5+} and Ga^{3+} ones are distributed over both the [B] and (C) sites, while Li^+ incorporation takes place only at the (C) sites. This determines the structure disorder leading to inhomogeneous spectral broadening for the active ions. The Rietveld refinement of the crystal structure indicates a very low content of cationic vacancies □ in the A and (C) sites (about 0.4%) which is an evidence for the positive role of charge compensators.

Let us describe briefly the spectroscopic properties of the Tm,Ho:LCLNGG crystal. Firstly, the transmission spectra of several Tm,Ho:CNGG-type crystals grown under identical conditions with similar doping (unmodified, containing only Li^+ cations and containing both La^{3+} and Li^+ cations) were measured in the visible, Fig. 1(a). The thickness of the studied samples was the same. For the last crystal, the broad absorption band underlying the bands due to RE^{3+} ions and originating from color centers has the lowest intensity. This indicates the positive role of introducing both the La^{3+} and Li^+ charge compensators.

The Li^+ cations reduce the vacancies only at the tetrahedral sites (C) which they occupy. As for the La^{3+} cations, together with other two RE^{3+} (Tm^{3+}, Ho^{3+}) ions they substitute for the Ca^{2+} ions in the dodecahedral sites (A). This substitution is expected to reduce the lattice tension and vacancies in the (A) sites. The ionic radii of laser-active Tm^{3+} and Ho^{3+} dopants for VIII-fold oxygen coordination ($R_{Tm} = 0.994$ Å and $R_{Ho} = 1.015$ Å) are smaller than that of the host-forming Ca^{2+} cations ($R_{Ca} = 1.12$ Å). A substitution of $1Ca^{2+}$ by $1Tm^{3+}|Ho^{3+}$ requires a vacancy □ and causes a significant lattice tension. The La^{3+} ions are relatively big ($R_{La} = 1.16$ Å), so that during the substitution, e.g., of $3Ca^{2+}$ by $1La^{3+}$ and $1Tm^{3+}$, the lattice tension is reduced and no vacancy is involved. Thus, the introduction of Li^+ and La^{3+} decreases the vacancies in the (C) and (A) sites, respectively, thus improving the material crystallinity and its optical quality.

Figure 1(b) shows the absorption band related to the $^3H_6 \rightarrow {}^3H_4$ transition of Tm^{3+} ions in LCLNGG. The maximum absorption cross-section σ_{abs} is 0.92×10^{-20} cm^2 at 801.0 nm and the absorption bandwidth is ~27 nm. This indicates the suitability of this crystal for pumping with AlGaAs-based diode lasers. The emission spectrum of the Tm,Ho:LCLNGG crystal at ~2 μm is

Optics EXPRESS

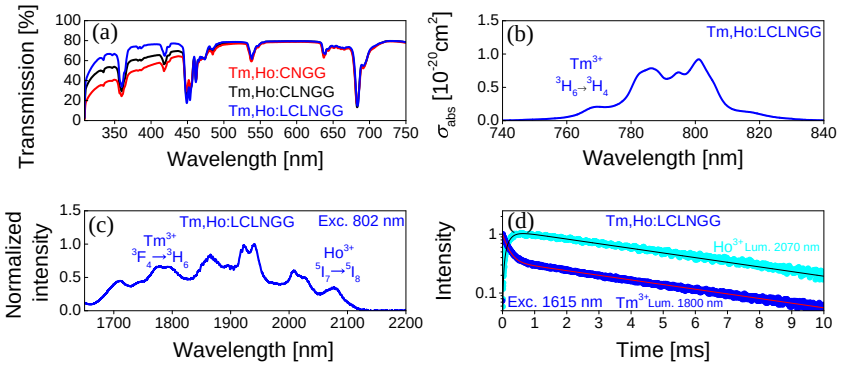

Fig. 1. Optical spectroscopy of the Tm,Ho:LCLNGG crystal: (a) transmission spectrum in the visible, the spectra for Tm,Ho:CNGG and Tm:CLNGG crystals are given for comparison; (b) absorption cross-section, σ_{abs}, corresponding to the $^3H_6 \rightarrow {}^3H_4$ Tm^{3+} transition; (c) luminescence spectrum at ~2 μm, $\lambda_{exc} = 802$ nm; (d) luminescence decay curves for Tm^{3+} (1800nm) and Ho^{3+} (2070nm) emissions, $\lambda_{exc} = 1615$ nm.

presented in Fig. 1(c). The composite luminescence is due to the spectrally overlapping $^3F_4 \rightarrow {}^3H_6$ Tm^{3+} and $^5I_7 \rightarrow {}^5I_8$ Ho^{3+} transitions. The spectrum is smooth and broad spanning up to ~2.15 μm. In the long-wave part of the emission spectrum where laser operation is expected (considering the quasi-three-level laser schemes), a broad peak centered at ~2.07 μm is observed. Such emission properties are attractive for the design of ML lasers.

The luminescence decay from both ions was studied under resonant excitation of the Tm^{3+} ions, Fig. 1(d). The decay curves reveal an efficient and predominantly unidirectional $Tm^{3+} \rightarrow Ho^{3+}$ energy transfer. The thermal equilibrium decay time τ_0 for both the $^3F_4$ Tm^{3+} and $^5I_7$ Ho^{3+} multiplets is 5.5 ± 0.2 ms.

3. Experimental configuration

A scheme of the Tm,Ho:LCLNGG laser is shown in Fig. 2. An X-shaped astigmatically compensated linear cavity was employed for evaluating both the CW and passively ML laser performance. The rectangular active element was cut from the 2.02 at.% Tm^{3+}, 0.36 at.% Ho^{3+}:LCLNGG crystal along the crystallographic [111] direction. It had an aperture of 3 mm × 3 mm and a thickness of 3 mm. The active element was polished to laser quality from both sides and left uncoated. It was mounted in a water-cooled Cu holder (coolant temperature: 14°C) and placed at Brewster's angle between two dichroic folding mirrors M_1 and M_2 (radius of curvature: RoC = −100 mm). The pump source was a CW Ti:Sapphire laser tuned to the absorption maximum. It was focused into the crystal with a spherical focusing lens ($f = 70$ mm) yielding an estimated waist radius of ~30 μm × 57 μm in the sagittal and tangential planes, respectively. A Lyot filter (3.2-mm thick quartz plate) was inserted at Brewster's angle close to the output coupler (OC) for wavelength tuning in the CW regime.

A transmission-type SWCNT-SA was used in the mode-locking experiments to initiate and stabilize the soliton pulse shaping. It was inserted in the second beam waist formed by the concave M_4 (RoC = −100 mm) and M_5 (RoC = −50 mm) mirrors. The SA comprised an uncoated ~1 mm-thick quartz substrate with a SWCNT/PMMA composite film on it deposited by spin coating. The diameters of the purified SWCNTs synthesized by the dried arc-discharge method were selected to provide a broad absorption band spanning from 1.9 to 2.1 μm due to the first fundamental transition of the semiconducting nanotubes, E_{11}. The absorption saturation properties for normal incidence were the following: a modulation depth <0.5%, a non-saturable

Optics EXPRESS

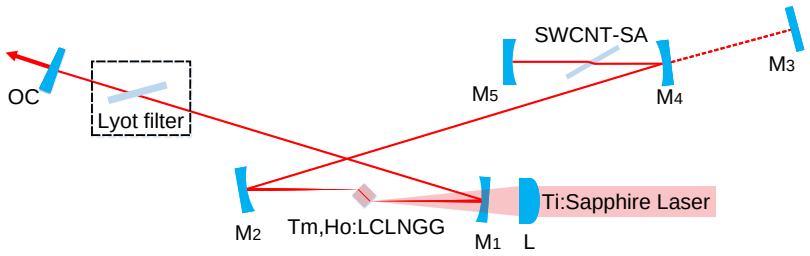

Fig. 2. Scheme of the Tm,Ho:LCLNGG laser: L: spherical focusing lens ($f = 70$ mm); M_1-M_2: concave mirrors (RoC = −100 mm), M_3: flat rear mirror for CW operation; M_4: concave mirror (RoC = −100 mm); M_5: concave mirror (RoC = −50 mm); OC: output coupler; SWCNT-SA: single-walled carbon nanotube saturable absorber.

loss of 1% and a saturation fluence about 10 μJ/cm^2. The recovery time of the initial absorption at ~2 μm was ~1 ps [21].The intracavity group delay dispersion (GDD) was managed by broadband dispersive mirrors (DMs) exhibiting negative GDD of −125 fs^2 per bounce and more than 300 nm reflectivity bandwidth from 1850 to 2150 nm.

4. Experimental results

4.1. CW laser operation

The CW laser performance of the Tm,Ho:LCLNGG crystal was first investigated with a four-mirror laser cavity including a plane rear reflector M_3 and a plane-wedged OC (without the SA). Four OCs with transmission T_{OC} in the range of 0.2% - 3% were used. The radius of the laser mode in the crystal was estimated using the ABCD formalism yielding 23 μm × 46 μm in the sagittal and tangential planes, respectively. The measured single-pass pump absorption under lasing conditions was dependent on the output coupling and amounted to 48.2% for 1.5% OC, revealing some absorption bleaching.

A maximum CW output power of 350 mW was obtained at 2080.5 nm for an absorbed pump power of 1.54 W, corresponding to a laser threshold of 92.8 mW and a slope efficiency of 23.8% with respect to the pump power absorbed in the crystal ($T_{OC} = 1.5\%$), see Fig. 3(a). The laser threshold gradually increased with the output coupling, from 70.2 mW for 0.2% OC to 108.8 mW for 3% OC. The emission wavelength experienced a blue-shift with T_{OC}, from 2085.4 nm for 0.2% OC to 2075.1 nm for 3% OC. This behavior is due to the quasi-three-level nature of the $^5I_7 \rightarrow {}^5I_8$ Ho^{3+} transition. The laser operated solely on the Ho^{3+} laser transition, no Tm^{3+} co-lasing was detected. The Lyot filter was inserted for wavelength tuning in the CW regime. With the 0.5% OC, a relatively broad range of continuous wavelength tuning, ~210 nm (1904.1–2114.1 nm) was achieved at an absorbed pump power of 1.04 W, see Fig. 3(b). The maximum output power was obtained at the wavelength of 2085.4 nm.

The Caird analysis [22] was applied to estimate the total passive losses δ (including cavity and laser crystal but excluding the reabsorption effect) and the intrinsic slope efficiency η_0 through fitting the measured laser slope efficiency as a function of the reflectivity of the OC, $R_{OC} = 1 - T_{OC}$. The best fit gave round trip cavity losses of $\delta = 0.3 \pm 0.1\%$ and an intrinsic slope efficiency of $\eta_0 = 27.4\%$, see Fig. 3(c).

4.2. Soliton ML operation

For mode-locking, the SWCNT-SA was placed in the second beam waist created by the M_4 and M_5 mirrors and inclined at Brewster's angle. The beam radius at the SA was estimated by the ABCD formalism to be 149 μm × 214 μm in the sagittal and tangential planes, respectively. To

Optics EXPRESS

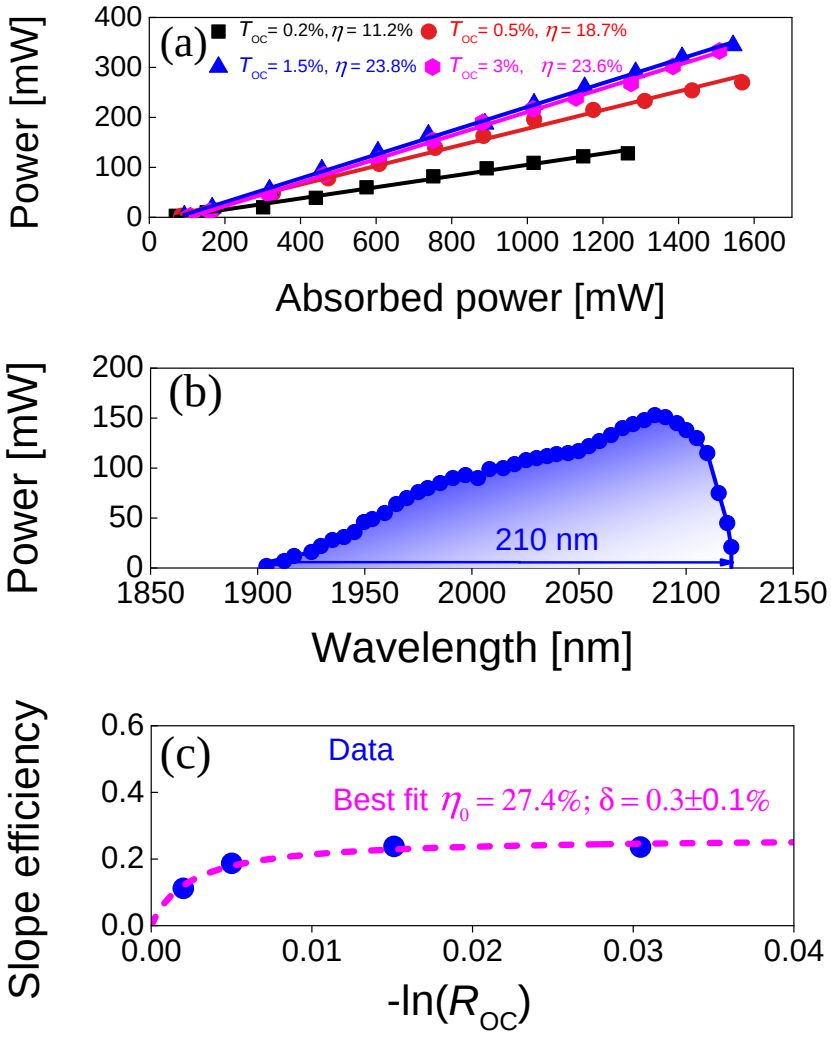

Fig. 3. CW Tm,Ho:LCLNGG laser: (a) input-output dependences for different OCs, η - slope efficiency; (b) spectral tuning range obtained with a Lyot filter, P_{abs} = 1.04 W, T_{OC} = 0.5%; (c) evaluation of the passive losses using the Caird approach.

Optics EXPRESS

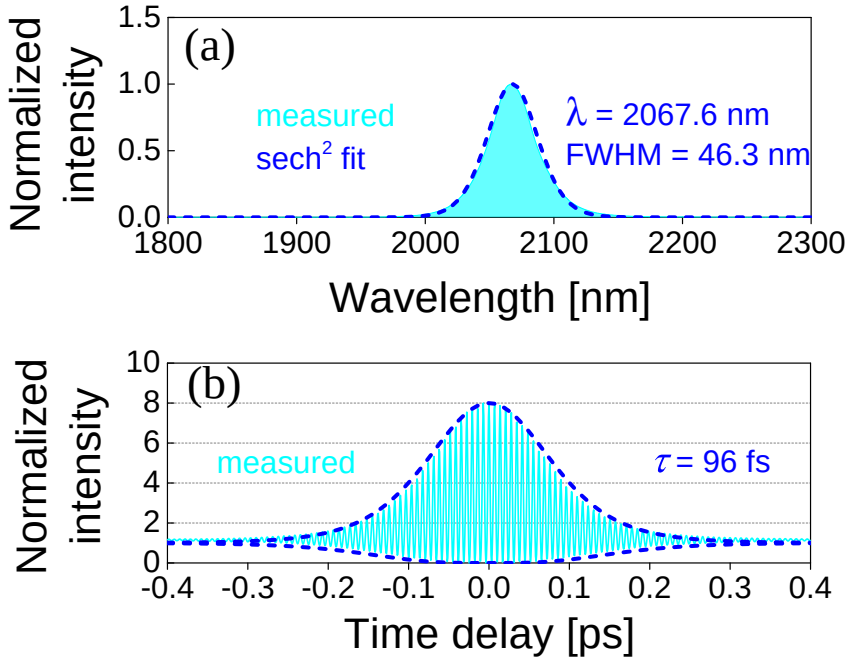

Fig. 4. ML Tm,Ho:LCLNGG laser with $T_{OC} = 1.5\%$: (a) optical spectrum; (b) interferometric autocorrelation trace.

balance the self-phase modulation (SPM) inducing a positive frequency chirp and to ensure efficient soliton pulse shaping, the M_4 mirror was replaced by a concave DM_1 (RoC = −100 mm, GDD = −125 fs^2 per bounce) resulting in a total round-trip GDD of −250 fs^2, see Fig. 2. Firstly, by applying the 1.5% OC, self-starting ML operation was achieved. The measured spectrum and the fringe-resolved autocorrelation trace gave a pulse duration of 96 fs at a central wavelength of 2067.6 nm and a spectral bandwidth (determined at full width at half maximum, FWHM) of 46.3 nm assuming sech^2-shaped spectral and temporal profiles, see Fig. 4. The resulting time-bandwidth product (TBP) was 0.318, very close to the Fourier-transform limit for sech^2-shaped soliton pulses. The average output power from the ML laser amounted to 121 mW at an absorbed pump power of 1.59 W and the pulse repetition rate was ~102.5 MHz. Excellent sech^2-shaped spectral and temporal profiles of the generated pulses indicated efficient soliton ML operation of the Tm,Ho:LCLNGG laser.

The shortest pulse duration was achieved by employing a lower OC of 0.5%. The measured spectrum of the ML laser was centered at 2072.7 nm spanning from 1928 to 2234 nm, see Fig. 5(a). After external linear chirp compensation with a 3-mm thick ZnS ceramic plate, pulses as short as 63 fs were confirmed by an autocorrelation trace measurement. Note that the pulse duration of 63 fs was ~17% above the Fourier limit. The maximum average output power for the shortest pulses amounted to 63 mW at an absorbed pump power of 1.59 W with a pulse repetition rate of ~102.5 MHz.

The pulse train from the Tm,Ho:LCLNGG laser was characterized by a radio-frequency (RF) spectrum analyzer. The fundamental beat note was located at ~102.5 MHz (recorded with a resolution bandwidth, RBW = 100 Hz) and exhibited high extinction ratio of >82 dBc above the noise level, see Fig. 6(a). The measured uniform harmonic beat notes in a 2-GHz frequency span (RBW: 100 kHz) revealed highly stable steady-state CW mode-locking without any unwanted Q-switching or multi-pulsing instabilities, see Fig. 6(b).

Optics EXPRESS

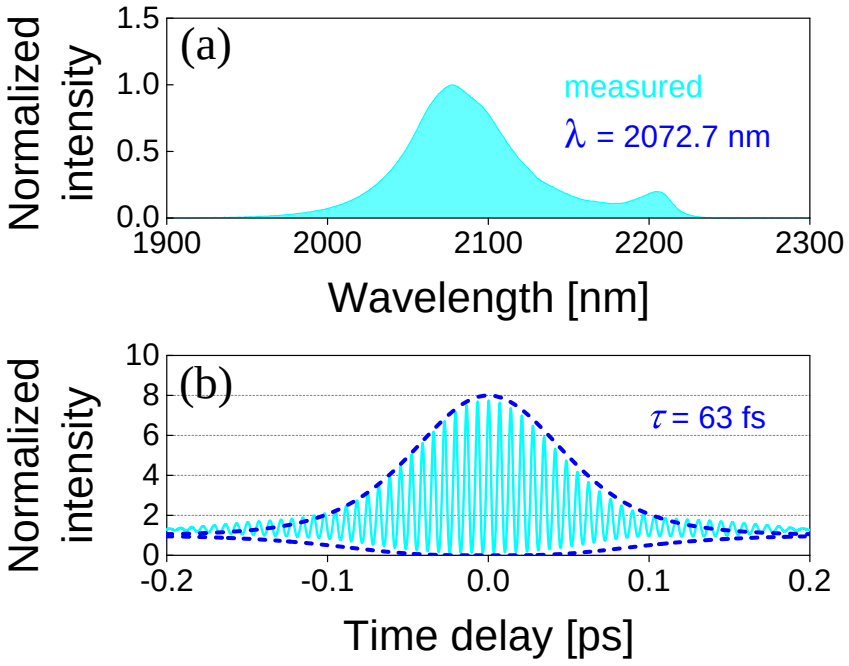

Fig. 5. ML Tm,Ho:LCLNGG laser with $T_{OC} = 0.5\%$. (a) optical spectrum; (b) interferometric autocorrelation trace.

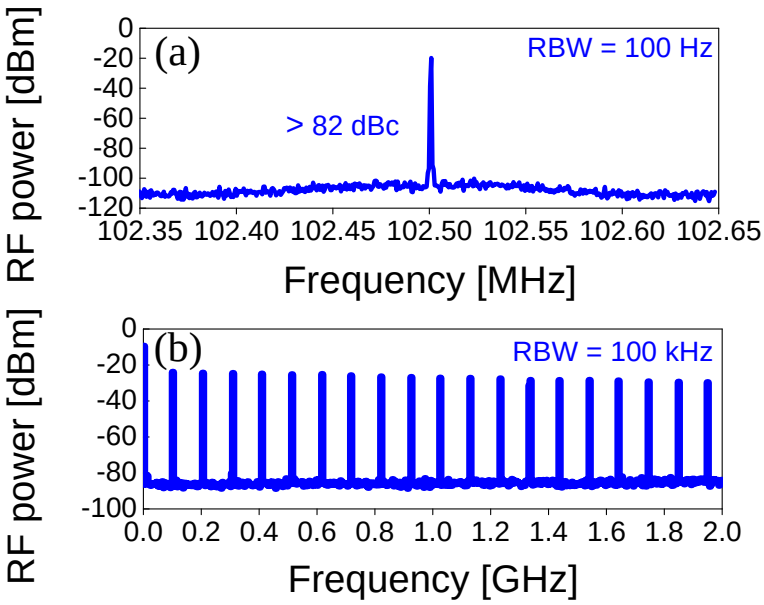

Fig. 6. RF spectra of the ML Tm,Ho:LCLNGG laser: (a) fundamental beat note and (b) 2-GHz span. RBW: resolution bandwidth.

Optics EXPRESS

5. Conclusion

To conclude, we have demonstrated the first passively ML Tm,Ho:LCLNGG laser with pulse durations in the sub-100 fs time domain. A transmission-type SWCNT-SA was implemented for initiating and stabilizing the soliton pulse shaping. Pulses as short as 63 fs were achieved at 2072.7 nm with an average output power of 63 mW at a pulse repetition rate of ~102.5 MHz. This result represents the shortest pulse ever achieved from a ML laser at ~2 μm based on Tm^{3+},Ho^{3+}-codoped cubic multicomponent garnets. The introduction of Li^{+} and La^{3+} in the structure reduces the vacancies and mosaicity in the crystal improving its quality and providing better laser performance. Higher average output power of 121 mW was obtained at the cost of longer pulse duration of 96 fs at 2067.6 nm. The relevant spectroscopic properties of this novel codoped CNGG-type garnet crystal, as well as the results of the present work, i.e., the broad tunability range and the generation of sub-100-fs pulses, indicate the potential of Tm,Ho:LCLNGG for the design of ultrafast (few optical cycle) power-scalable oscillators emitting at ~2 μm, pumped by commercial high-power diode lasers at ~800 nm.

Funding. National Natural Science Foundation of China (61975208, 51761135115, 61850410533, 62075090, 52032009, 52072351); Foundation of President of China Academy of Engineering Physics (YZJJLX2018005); Sino-German Scientist Cooperation and Exchanges Mobility Program (M-0040); Foundation of Key Laboratory of Optoelectronic Materials Chemistry and Physics, Chinese Academy of Sciences (2008DP173016); National Research Foundation of Korea (NRF-2020R1A4A2002828); Foundation of State Key Laboratory of Crystal Materials, Shandong University (KF2001).

Disclosures. The authors declare no conflicts of interest.

Data availability. Data underlying the results presented in this paper are not publicly available at this time but may be obtained from the authors upon reasonable request.

References

1. A. Schliesser, N. Picqué, and T. W. Hänsch, "Mid-infrared frequency combs," Nat. Photonics **6**(7), 440–449 (2012).
2. L. von Grafenstein, M. Bock, D. Ueberschaer, K. Zawilski, P. Schunemann, U. Griebner, and T. Elsaesser, "5 μm few-cycle pulses with multi-gigawatt peak power at a 1 kHz repetition rate," Opt. Lett. **42**(19), 3796–3799 (2017).
3. L. von Grafenstein, M. Bock, D. Ueberschaer, A. Koç, U. Griebner, and T. Elsaesser, "2.05 μm chirped pulse amplification system at a 1 kHz repetition rate-2.4 ps pulses with 17 GW peak power," Opt. Lett. **45**(14), 3836–3839 (2020).
4. A. Schmidt, S. Y. Choi, D. I. Yeom, F. Rotermund, X. Mateos, M. Segura, F. Diaz, V. Petrov, and U. Griebner, "Femtosecond pulses near 2 μm from a Tm:KLuW laser mode-locked by a single-walled carbon nanotube saturable absorber," Appl. Phys. Express **5**(9), 092704 (2012).
5. Y. Wang, Y. Zhao, Z. Pan, J. E. Bae, S. Y. Choi, F. Rotermund, P. Loiko, J. M. Serres, X. Mateos, H. Yu, H. Zhang, M. Mero, U. Griebner, and V. Petrov, "78 fs SWCNT-SA mode-locked Tm:CLNGG disordered garnet crystal laser at 2017nm," Opt. Lett. **43**(17), 4268–4271 (2018).
6. Z. Pan, Y. Wang, Y. Zhao, H. Yuan, X. Dai, H. Cai, J. E. Bae, S. Y. Choi, F. Rotermund, X. Mateos, J. M. Serres, P. Loiko, U. Griebner, and V. Petrov, "Generation of 84-fs pulses from a mode-locked Tm:CNNGG disordered garnet crystal laser," Photonics Res. **6**(8), 800–804 (2018).
7. Y. Zhao, L. Wang, W. Chen, Z. Pan, Y. Wang, P. Liu, X. Xu, Y. Liu, D. Shen, J. Zhang, M. Guina, X. Mateos, P. Loiko, Z. Wang, X. Xu, J. Xu, M. Mero, U. Griebner, and V. Petrov, "SESAM mode-locked Tm:$LuYO_3$ ceramic laser generating 54-fs pulses at 2048nm," Appl. Opt. **59**(33), 10493–10497 (2020).
8. Y. Zhao, L. Wang, Y. Wang, J. Zhang, P. Liu, X. Xu, Y. Liu, D. Shen, J. E. Bae, T. G. Park, F. Rotermund, X. Mateos, P. Loiko, Z. Wang, X. Xu, J. Xu, M. Mero, U. Griebner, V. Petrov, and W. Chen, "SWCNT-SA mode-locked Tm:$LuYO_3$ ceramic laser delivering 8-optical-cycle pulses at 2.05 μm," Opt. Lett. **45**(2), 459–462 (2020).
9. Y. Zhao, L. Wang, W. Chen, P. Loiko, Y. Wang, Z. Pan, H. Yang, W. Jing, H. Huang, J. Liu, X. Mateos, Z. Wang, X. Xu, U. Griebner, and V. Petrov, "Kerr-lens mode-locked Tm-doped sesquioxide ceramic laser," Opt. Lett. **46**(14), 3428–3431 (2021).
10. A. Suzuki, C. Kränkel, and M. Tokurakawa, "Sub-6 optical-cycle Kerr-lens mode-locked Tm:Lu_2O_3 and Tm:Sc_2O_3 combined gain media laser at 2.1 μm," Opt. Express **29**(13), 19465–19471 (2021).
11. Y. Zhao, Y. Wang, X. Zhang, X. Mateos, Z. Pan, P. Loiko, W. Zhou, X. Xu, J. Xu, D. Shen, S. Suomalainen, A. Härkönen, M. Guina, U. Griebner, and V. Petrov, "87 fs mode-locked Tm,Ho:$CaYAlO_4$ laser at ~2043nm," Opt. Lett. **43**(4), 915–918 (2018).
12. V. Petrov, Y. Wang, W. Chen, Z. Pan, Y. Zhao, L. Wang, M. Mero, S. Y. Choi, F. Rotermund, W. B. Cho, W. Jing, H. Huang, H. Yuan, H. Cai, L. Zhang, Z. Lin, P. Loiko, X. Mateos, X. Xu, J. Xu, H. Yu, H. Zhang, S. Suomalainen, M. Guina, A. Härkönen, and U. Griebner, "Sub-100-fs bulk solid-state lasers near 2-micron," Proc. SPIE **11209**, 214 (2019).

Optics EXPRESS

13. L. Wang, W. Chen, Y. Zhao, P. Loiko, X. Mateos, M. Guina, Z. Pan, M. Mero, U. Griebner, and V. Petrov, "Sub-50 fs pulse generation from a SESAM mode-locked Tm,Ho-codoped calcium aluminate laser," Opt. Lett. **46**(11), 2642–2645 (2021).
14. J. Ma, Z. Pan, J. Wang, H. Yuan, H. Cai, G. Xie, L. Qian, D. Shen, and D. Tang, "Generation of sub-50 fs soliton pulses from a mode-locked Yb,Na:CNGG disordered crystal laser," Opt. Express **25**(13), 14968–14973 (2017).
15. G. Xie, D. Tang, W. Tan, H. Luo, H. Zhang, H. Yu, and J. Wang, "Subpicosecond pulse generation from a Nd:CLNGG disordered crystal laser," Opt. Lett. **34**(1), 103–105 (2009).
16. L. Wang, W. Chen, Z. Pan, P. Loiko, J. E. Bae, F. Rotermund, X. Mateos, U. Griebner, and V. Petrov, "Sub-100 fs mode-locked Tm:CLTGG laser," Opt. Express **29**(20), 31137–31144 (2021).
17. Z. Pan, J. M. Serres, E. Kifle, P. Loiko, H. Yuan, X. Dai, H. Cai, M. Aguiló, F. Díaz, Y. Wang, Y. Zhao, U. Griebner, V. Petrov, and X. Mateos, "Comparative study of the spectroscopic and laser properties of Tm^{3+}, Na^{+}(Li^{+})-codoped $Ca_3Nb_{1.5}Ga_{3.5}O_{12}$-type disordered garnet crystals for mode-locked lasers," Opt. Mater. Express **8**(8), 2287–2299 (2018).
18. Z. Pan, P. Loiko, Y. Wang, Y. Zhao, H. Yuan, K. Tang, X. Dai, H. Cai, J. M. Serres, S. Slimi, E. Ben Salem, E. Dunina, A. Kornienko, L. Fomicheva, J.-L. Doualan, P. Camy, W. Chen, U. Griebner, V. Petrov, M. Aguiló, F. Díaz, R. M. Solé, and X. Mateos, "Disordered Tm^{3+},Ho^{3+}-codoped CNGG garnet crystal: Towards efficient laser materials for ultrashort pulse generation at ~2 μm," J. Alloy. Compd. **853**, 157100 (2021).
19. Z. Pan, Y. Wang, Y. Zhao, M. Kowalczyk, J. Sotor, H. Yuan, Y. Zhang, X. Dai, H. Cai, J. E. Bae, S. Y. Choi, F. Rotermund, P. Loiko, J. M. Serres, X. Mateos, U. Griebner, and V. Petrov, "Sub-80 fs mode-locked Tm,Ho-codoped disordered garnet crystal oscillator operating at 2081nm," Opt. Lett. **43**(20), 5154–5157 (2018).
20. Y. Zhao, Y. Wang, W. Chen, Z. Pan, L. Wang, X. Dai, H. Yuan, Y. Zhang, H. Cai, J. E. Bae, S. Y. Choi, F. Rotermund, P. Loiko, J. M. Serres, X. Mateos, W. Zhou, D. Shen, U. Griebner, and V. Petrov, "67-fs pulse generation from a mode-locked Tm,Ho:CLNGG laser at 2083nm," Opt. Express **27**(3), 1922–1928 (2019).
21. W. B. Cho, J. H. Yim, S. Y. Choi, S. Lee, A. Schmidt, G. Steinmeyer, U. Griebner, V. Petrov, D. I. Yeom, K. Kim, and F. Rotermund, "Boosting the nonlinear optical response of carbon nanotube saturable absorbers for broadband mode-locking of bulk lasers," Adv. Funct. Mater. **20**(12), 1937–1943 (2010).
22. J. A. Caird, S. A. Payne, P. R. Staver, A. Ramponi, and L. Chase, "Quantum electronic properties of the $Na_3Ga_2Li_3F_{12}$:Cr^{3+} laser," IEEE J. Quantum Electron. **24**(6), 1077–1099 (1988).